APPLIED PHYSICS LETTERS **106**, 161101 (2015)

Thermal characterisation of (bio)polymers with a temperature-stabilised whispering gallery mode microsensor

Eugene Kim, Matthew R. Foreman, Martin D. Baaske, and Frank Vollmer[a)]
Max Planck Institute for the Science of Light, Günther-Scharowsky-Straße 1, 91058 Erlangen, Germany

(Received 23 March 2015; accepted 12 April 2015; published online 20 April 2015)

In this work, we theoretically and experimentally investigate the thermal response of whispering gallery mode microresonators operating in an aqueous glycerol medium. Thermal stabilisation of the resonance wavelength is realised by appropriate choice of the resonator radius and glycerol concentration, with a 60 fold reduction in thermal sensitivity demonstrated. Finally, we employ our stabilised system to determine the thermal dependence of the molecular polarisability of adsorbed bovine serum albumin molecules and the refractive index of dextran and poly(diallyldimethylammonium chloride) coatings. *© 2015 AIP Publishing LLC*. [http://dx.doi.org/10.1063/1.4918932]

Whispering gallery mode (WGM) resonators have emerged as a powerful platform for miniaturised label-free biosensors in recent years.[1–5] Light in WGM resonators can circulate around the surface for a long time (i.e., as a high Q mode) and with high local field intensities, therefore, allowing a strong interaction with matter near the surface. These properties afford extreme levels of sensitivity down to detection of individual nanoparticles and biomolecules, such as viruses,[1] proteins,[2] and DNA strands.[3] Frequently, the operational principle of WGM biosensors is based on monitoring reactive resonance shifts induced upon binding of molecules of interest. An important drawback of this method, however, is that the resonance shift is not only sensitive to analyte molecules but also to local environmental perturbations, such as changes in the ambient pressure, mechanical vibrations, and temperature fluctuations which, in turn, limit the sensitivity of the sensor.[6] Of these detrimental influences, thermal effects, which can manifest as a distortion of the Lorentzian lineshape,[7] an increased noise floor,[8] or a continuous long term drift, is frequently most significant. A number of strategies to reduce or eliminate thermal perturbations of WGM resonators have previously been proposed, including optical,[9–12] material,[13–17] and geometric approaches.[6,13,18] In this work, we propose a complementary hybrid geometric-material based method for thermal stabilisation of spherical microresonators. Specifically, we theoretically and experimentally investigate compensation of temperature induced resonance shifts by controlling the radius, R, of the WGM resonator and the thermal refractive coefficient dn_h/dT of the host medium (where n_h and T denote the refractive index of the host medium and ambient temperature, respectively) by use of aqueous glycerol solutions. Notably, our method does not require high fabrication precision as demanded by other coating based techniques[14,16] and furthermore maintains biocompatibility of the sensing environment.[19] Through temperature stabilisation, we render the previously unresolvable temperature response of adsorbed molecules detectable. To demonstrate this potential, we investigate the thermal response of three different (bio)polymers, namely, bovine serum albumin (BSA), dextran, and poly(diallyldimethylammonium chloride) (polyDADMAC).

The thermal sensitivity of WGMs, as characterised by the rate at which the resonance wavelength, λ, varies with temperature (i.e., $d\lambda/dT$), can be derived from the underlying resonance condition. Assuming a spherical resonator of refractive index n_r, standard Mie theoretic derivations give the resonance condition as[5]

$$\frac{[n_h x\, y_l(n_h x)]'}{y_l(n_h x)} = N\,\frac{[n_r x\, j_l(n_r x)]'}{j_l(n_r x)}, \tag{1}$$

where $N = 1$ or $n_h^2/n_r^2 = 1/m^2$ for transverse electric (TE) or transverse magnetic (TM) modes respectively, $j_l(x)$ and $y_l(x)$ are the spherical Bessel functions of the first and second kind, $x = 2\pi R/\lambda$, and the prime notation denotes differentiation with respect to the argument of the Bessel functions. Differentiation of Eq. (1) with respect to T yields an equation from which $d\lambda/dT$ can be found. Frequently in the literature, however, an approximate asymptotic resonance formula, first derived by Lam *et al.*[20] (and henceforth referred to as the Lam approximation), is used. The thermal sensitivity again follows through differentiation and is approximately given by:

$$n_r x\left[\frac{1}{\lambda}\frac{d\lambda}{dT} + \frac{1}{R}\frac{dR}{dT} + \frac{1}{n_r}\frac{dn_r}{dT}\right] = \frac{M}{(m^2-1)^{3/2}}\frac{dm}{dT}, \tag{2}$$

where $M = 1$ and $(2m^2-1)/m^2$ for TE and TM modes, respectively. Thermal expansion of the resonator, as described by the expansion coefficient $R^{-1}dR/dT$, hence also plays a role in dictating thermal sensitivities. Note that $dm/dT = [n_h dn_r/dT - n_r dn_h/dT]/n_h^2$ and thus depends on the properties of both the resonator and host medium. For a fused silica resonator, both the thermal refractive and expansion coefficients are positive (11.9×10^{-6} K^{-1} and 5.5×10^{-7} K^{-1} respectively[15]) leading to a red-shift of the resonance for increasing temperatures when the resonator is in air ($dn_h/dT = 0$). Biosensing, however, practically must be performed in an aqueous medium such that dn_h/dT must also be considered. Although pure water possesses a negative thermal refractive coefficient of -8.36×10^{-5} K^{-1}, its magnitude is insufficient to compensate for the response of the resonator except for small lossy resonators which are unsuitable for

---

[a)] Electronic mail: frank.vollmer@mpl.mpg.de

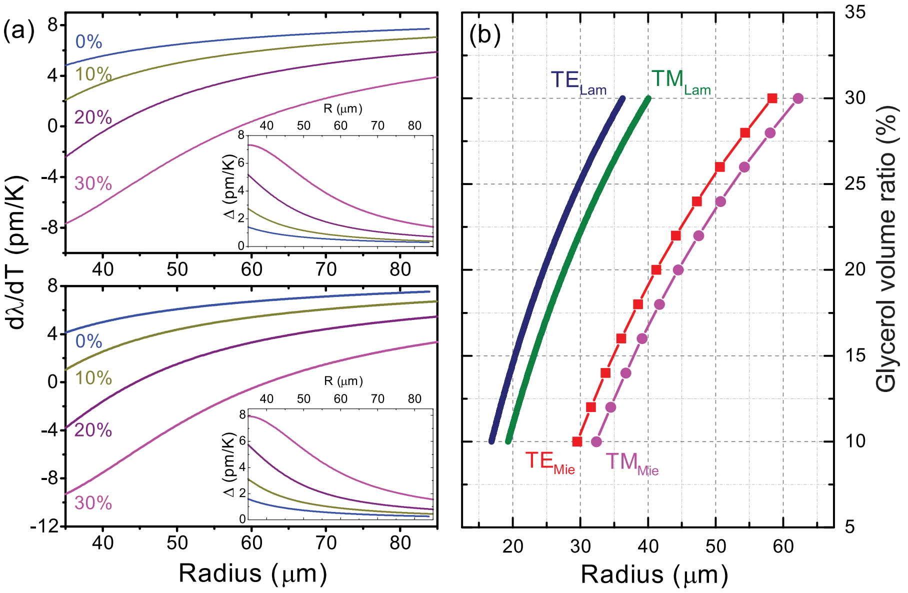

FIG. 1. (a) Numerical thermal sensitivities as a function of resonator radius for TE (top) and TM (bottom) WGMs and various glycerol volume concentrations as found using Mie theory (main panel). Insets depict the difference between the Mie solution and Lam approximation ($\Delta = (d\lambda/dT)_{\mathrm{Lam}} - (d\lambda/dT)_{\mathrm{Mie}}$). (b) Resonator radius required to achieve zero thermal response as a function of glycerol concentration found using both Mie and Lam solutions.

high sensitivity biosensing. In order to further increase the magnitude of dn_h/dT without adversely affecting biomolecular function of potential adsorbates, we add glycerol to the water. The effective refractive index of the host medium then follows as a weighted average of the refractive index of water (n_w) and glycerol (n_g), i.e., $n_h = f_g n_g + f_w n_w$, where f_g and f_w are the respective weight fractions,[21] such that:

$$\frac{dn_h}{dT} = f_g \frac{dn_g}{dT} + f_w \frac{dn_w}{dT}. \tag{3}$$

Fig. 1(a) shows $d\lambda/dT$ as found using the full Mie solution and the resulting difference with the Lam approximation. In general, the thermal sensitivity of WGM microspheres decreases with decreasing resonator size and as the glycerol:water ratio increases. The former occurs since in smaller resonators a larger fraction of the WGM extends beyond the resonator thereby increasing the total interaction with the host medium.[22] From Fig. 1, it is also evident that the Lam approximation underestimates the influence of the host medium, with larger discrepancies seen for smaller spheres. This behaviour derives from the underlying assumptions of the asymptotic expansion.[23] Nevertheless, the Mie calculations show that a zero thermal sensitivity is achievable for spheres of ~30–60 μm radius, using glycerol concentrations of 10–30 v/v % (Fig. 1(b)).

In light of these predictions, experimental verification was sought. The experimental setup used is shown in Fig. 2(a). WGMs were excited in a fused silica microsphere through a tapered fibre by sweeping the wavelength of a distributed feedback (DFB) laser ($\lambda \approx 1060$ nm) at a rate of 100 Hz. A thermoelectric cooler (TEC) used for heating and cooling was attached to the bottom of a polydimethylsiloxane (PDMS) liquid chamber into which the tapered fiber and

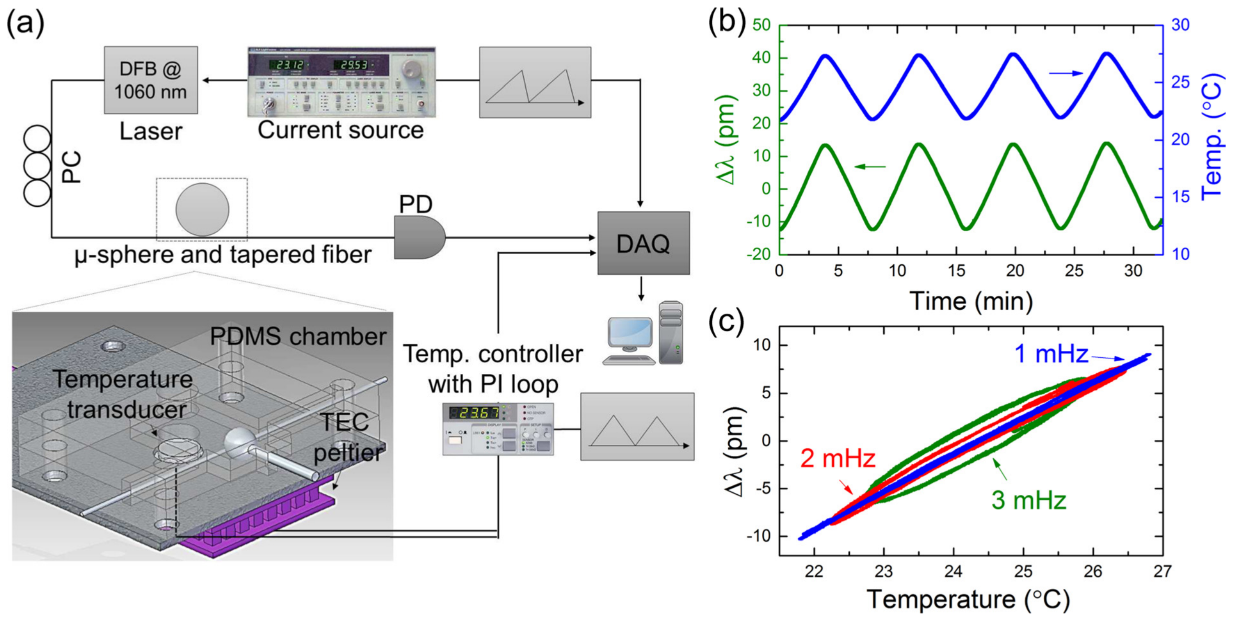

FIG. 2. (a) Schematic of the temperature controlled WGM setup. (b) Typical example of temperature and resonance traces during thermal cycling (taken from a $R = 38\,\mu$m sphere in water). (c) Resonance shift $\Delta\lambda$ versus T for different thermal cycling rates exhibiting hysteresis for rates above 1 mHz.

microsphere were immersed. The liquid chamber was sealed during measurements to prevent evaporation and thus maintain a constant glycerol:water ratio. A temperature transducer (with ±0.01 K resolution) was placed in the vicinity of the sphere to provide feedback to the TEC through a Proportional Integral loop. Both the temperature and the fibre transmission were recorded simultaneously. To extract values of $d\lambda/dT$, we actively cycled the temperature of the chamber over a 5 ± 1 K range at a rate of 1.2 ± 0.36 K/min for 3 to 5 cycles using the TEC and a signal generator. Cycling of the temperature, as opposed to a linear ramp, allowed possible resonance shifts induced from other sources, such as external temperature drifts, to be more easily removed in post processing. Typical traces of the temperature and resonance shift during thermal cycling are shown in Fig. 2(b). Importantly, a thermal cycling rate of ≤ 1 mHz was used to ensure that cycling was adiabatic. Faster cycling rates gave rise to a detrimental thermal hysteresis, as shown in Fig. 2(c).

Experimental thermal sensitivities ($d\lambda/dT$) for WGM resonators of varying radii are shown in Fig. 3 along with values found using Mie theory. Good agreement is seen over a large range of sizes; however, minor disagreement for $R \lesssim 36$ μm (Figs. 3(a) and 3(b)) is evident. Such discrepancies are attributed to non-sphericity of our resonators which is more significant for smaller spheres due to relatively larger distortions from the supporting stem. Moreover, experimental data likely include higher radial order WGMs (which exhibit a weaker dependence on the surrounding environment because a greater proportion of the mode lies within the resonator) since the typical free spectral range of our resonators (~1.6–4 nm) is larger than the laser scanning range (460 pm). Each data point in Fig. 3 corresponds to experimental data from an individual WGM resonance. Error bars reflect the precision of the conversion from applied laser sweeping voltage to laser wavelength, as found using an in-built interferometer. The precision to which $d\lambda/dT = 0$ can be achieved is practically limited by delivery of the correct concentration of glycerol. The smallest magnitude thermal sensitivity we achieved was 0.15 pm/K (in a 30% glycerol aqueous medium, $R = 62$ μm sphere), which represents a 60 (46) fold reduction as compared to a bare resonator in air (pure water). Finally, we note that whilst the proposed method functions by lowering dn_h/dT, it also increases n_h. Consequently, the reduced refractive index contrast causes increased radiative losses and a corresponding linewidth broadening, as depicted by the line plot in the inset of Fig. 3. Experimental measurements for a $R = 70$ μm sphere are also shown. Differences are attributed to the relative absorption properties of glycerol and water which play a key role in determining WGM linewidth.

Reduction of the thermal sensitivity of WGM resonators affords new opportunities in studies of the thermal response of molecules (as characterised by $d\alpha/dT$, where α is the excess polarisability of the molecule) or thin adsorbed layers (dn_l/dT). Without such thermal compensation techniques, the comparatively small thermal response of adsorbates cannot be easily resolved within larger resonance shifts arising from the material properties of the resonator and host medium. To demonstrate this potential, we have thermally characterised three (bio)polymers: BSA, dextran, and polyDADMAC. We recall that the resonance shift, $\Delta\lambda$, upon binding of molecules to a WGM resonator can be expressed (restricting to TE modes for simplicity) as[24]

$$\frac{\Delta\lambda}{\lambda} \approx \frac{\sigma\alpha}{\epsilon_0 (n_r^2 - n_h^2) R}, \tag{4}$$

where σ describes the surface density of adsorbed molecules and ϵ_0 is the permittivity of free space. Using known properties of BSA[25] and the measured binding shift upon saturation (Fig. 4(a)), we estimate a surface coverage of ≈0.23. When the surface coverage of absorbed molecules is sufficient such

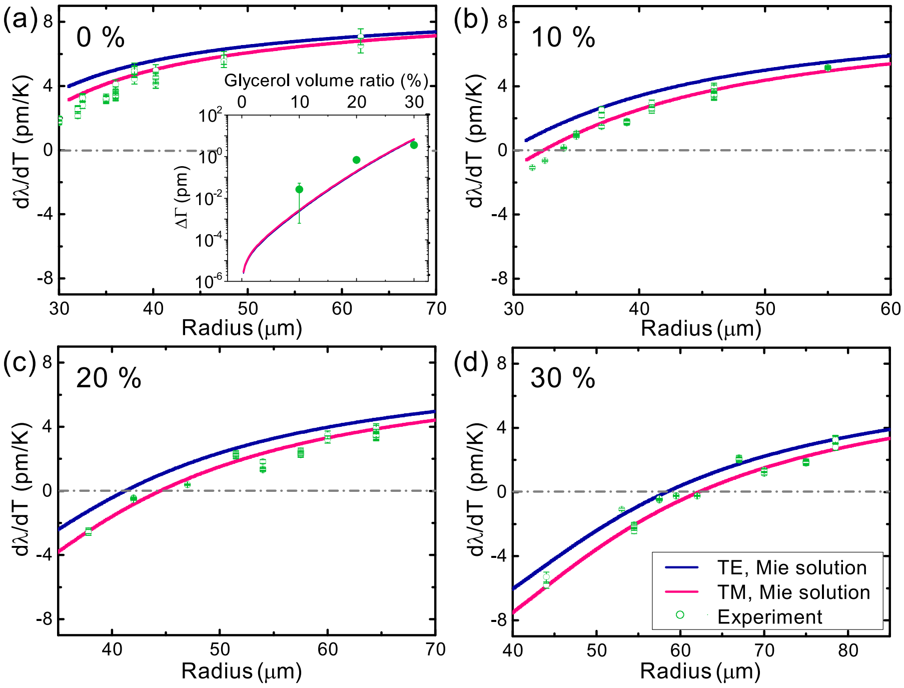

FIG. 3. Experimental (circles) and theoretical (solid lines) thermal sensitivities vs. resonator size for glycerol concentrations of (a) 0%, (b) 10%, (c) 20%, and (d) 30% by volume. Dashed-dotted lines depict zero thermal response. Inset shows the experimental (circles) and theoretical (solid line) broadening ($\Delta\Gamma = \Gamma - \Gamma_0$) of a 70 μm sphere vs. glycerol volume concentration. Theoretical plots are for radiative losses only.

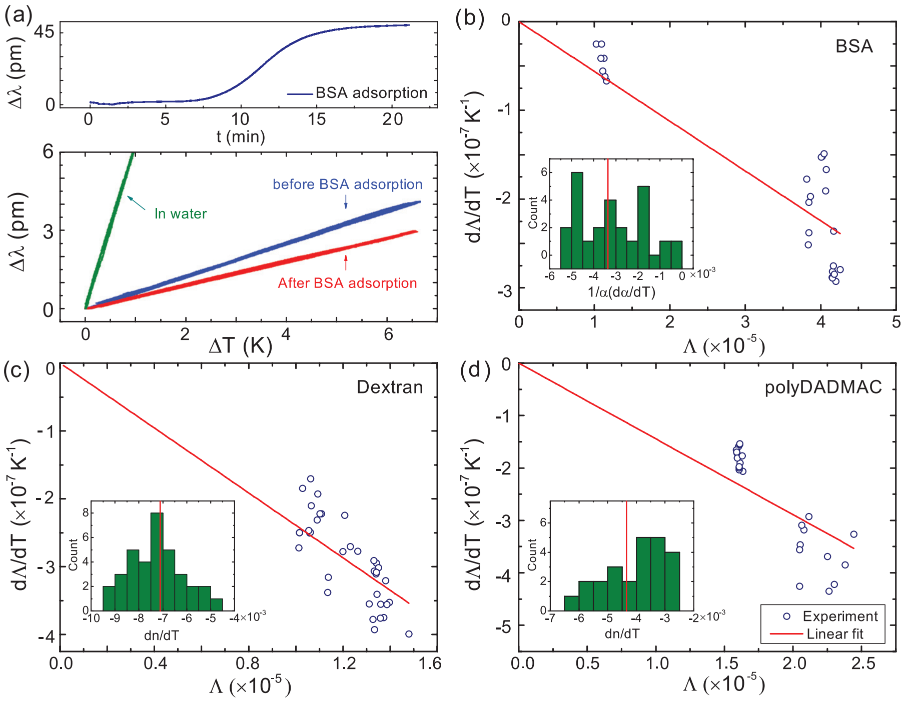

FIG. 4. (a) Standard binding curve obtained for BSA (top). (Bottom) Measured thermal response in water (green), water-glycerol mixture ∼30 v/v % (blue), and after subsequent binding of BSA (red). (b)–(d) Λ versus $d\Lambda/dT$ for BSA, dextran, and polyDADMAC, respectively. Red lines depict linear fits. Insets show histograms of $\alpha^{-1}d\alpha/dT$ and dn_l/dT values as compared to that found through fitting (red line).

that it appears as an optically contiguous layer, as is the case for dextran and polyDADMAC, we may treat it as a thin (mono)layer of thickness t and refractive index n_l, whereby[24]

$$\frac{\Delta\lambda}{\lambda} \approx \frac{n_l^2 - n_h^2}{n_r^2 - n_h^2}\frac{ft}{R}, \tag{5}$$

where f is the volume fraction of the layer comprised the adsorbate. Letting $\Lambda = \Delta\lambda/\lambda$, it follows that for adsorbed molecules:

$$\frac{1}{\Lambda}\frac{d\Lambda}{dT} = \frac{1}{\alpha}\frac{d\alpha}{dT} - \frac{1}{R}\frac{dR}{dT} + \frac{2}{\Delta n_{rh}^2}\left[n_h\frac{dn_h}{dT} - n_r\frac{dn_r}{dT}\right], \tag{6}$$

where $\Delta n_{ij}^2 = n_i^2 - n_j^2$, or for thin layers

$$\begin{aligned}\frac{1}{\Lambda}\frac{d\Lambda}{dT} &= \frac{2n_l}{\Delta n_{lh}^2}\frac{dn_l}{dT} - \frac{1}{R}\frac{dR}{dT}\\ &\quad + \frac{2}{\Delta n_{rh}^2}\left[n_h\frac{\Delta n_{lr}^2}{\Delta n_{lh}^2}\frac{dn_h}{dT} - n_r\frac{dn_r}{dT}\right].\end{aligned} \tag{7}$$

We note that Eqs. (6) and (7) are equivalent when $\sigma\alpha/\epsilon_0 = f(n_l^2 - n_h^2)t$. Importantly, the right hand sides of Eqs. (6) and (7) only depend on the material properties of the resonator, host medium, and adsorbate and are thus constant for any given experiment. Consequently, upon determination of the ratio $\Lambda^{-1}d\Lambda/dT \approx \lambda^{-1}d\lambda/dT - \lambda_0^{-1}d\lambda_0/dT$, where λ_0 denotes the WGM wavelength before adsorption of the molecules/layer, either $d\alpha/dT$ or dn_l/dT can be easily found.

To experimentally determine Λ and $d\Lambda/dT$, we first minimised the thermal response of a $R \approx 60\,\mu$m resonator by injecting an adequate amount of glycerol (∼30%) into aqueous medium as described above. With these parameters, Q factors of $\sim 10^5$, limited by water absorption and coupling losses, were typically achievable. The resulting thermal response is depicted in Fig. 4(a) as compared to that without the glycerol additive. We note that no adsorption of glycerol to the resonator surface was observed. Adsorbate was then injected into the host medium with final concentration of $\approx 0.5\,\mu$M and the binding kinetics monitored (shown in Fig. 4(a) for BSA). Binding of adsorbate was induced electrostatically. For BSA, this required adjusting the pH of the medium to between 3.8 and 4.0, whereby the negative charge on the silica sphere was sufficient to induce binding of the positively charged BSA molecules. In the case of dextran, the resonator was aminosilanised, whereby the amine group on the silica surface binds to negatively charged dextran. No special treatment was required to induce binding of polyDADMAC since it is a cationic polymer possessing one positive charge per monomer. After saturation of the binding curve (Fig. 4(a)), we repeated the thermal response measurement yielding the lower red line in Fig. 4(a). Given the low concentration of injected polymers, the change in dn_h/dT from unadsorbed polymers is negligible. Figs. 4(b)–4(d) show the resulting plots of Λ versus $d\Lambda/dT$ for BSA, dextran, and polyDADMAC, respectively, together with a linear fit through the origin. For adsorption of BSA molecules, reduction of the pH of the host medium to 3.5 resulted in a four fold decrease in the equilibrium binding shift, in turn allowing a larger range of Λ to be probed and a more reliable fit to be obtained. Insets in Figs. 4(b)–4(d) show histograms of the $d\alpha/dT$ or dn_l/dT found using Eqs. (6) and (7) extracted for individual data points. Variance in the data is attributed to our experimental ambiguity of mode polarisation, variations in the BSA structure due to differing pH values, and polydisperse polymer chains. Linear fits yield $\alpha^{-1}d\alpha/dT = (-3.7\pm1.48) \times 10^{-3}$ K^{-1}, $dn_l/dT = (-7.3\pm1.10) \times 10^{-3}$ K^{-1}, and $dn_l/dT = (-4.3\pm1.07) \times 10^{-3}$ K^{-1} for BSA, dextran, and polyDADMAC, respectively. A negative thermal response is seen in each case. For BSA, this might be related to thermal unfolding of proteins.[26] The negative response of both dextran and polyDADMAC layers is in agreement with that seen in other polymers albeit our results show thermal coefficients which are an order of magnitude larger than typical values.[27] One potential source of this difference is higher polymer chain mobility in our experiments resulting from a lack of polymer crosslinking, as is common in more conventional measurement techniques.

In conclusion, we have demonstrated the thermal stabilisation of a WGM microresonator in aqueous media by means of tuning the glycerol content and resonator size. Reduction of the thermal sensitivity of the WGM system furthermore allowed for the thermal properties of adsorbed BSA and polymer layers to be studied. Our work, on one hand, affords the possibility of thermal characterisation of a given analyte through compensation of large background signals, whilst on the other hand also allows study of thermally induced biological processes which generally require large temperature gradients.

This work was funded by the Max Planck Society (E.K., M.D.B., and F.V.) and the Alexander von Humboldt Foundation (M.R.F.).

[1] F. Vollmer, S. Arnold, and D. Keng, Proc. Natl. Acad. Sci. U. S. A. **105**, 20701 (2008).
[2] V. R. Dantham, S. Holler, C. Barbre, D. Keng, V. Kolchenko, and S. Arnold, Nano Lett. **13**, 3347 (2013).
[3] M. D. Baaske, M. R. Foreman, and F. Vollmer, Nat. Nanotechnol. **9**, 933 (2014).
[4] Y. Wu, D. Y. Zhang, P. Yin, and F. Vollmer, Small **10**, 2067 (2014).
[5] M. R. Foreman, J. D. Swaim, and F. Vollmer, "Whispering gallery mode sensors," Adv. Opt. Photonics (in press).
[6] M. R. Foreman, W.-L. Jin, and F. Vollmer, Opt. Express **22**, 5491 (2014).
[7] T. Carmon, L. Yang, and K. J. Vahala, Opt. Express **12**, 4742 (2004).
[8] M. L. Gorodetsky and I. S. Grudinin, J. Opt. Soc. Am. B **21**, 697 (2004).
[9] I. Grudinin, H. Lee, T. Chen, and K. Vahala, Opt. Express **19**, 7365 (2011).
[10] J. Zhu, Ş. K. Özdemir, L. He, and L. Yang, Appl. Phys. Lett. **99**, 171101 (2011).
[11] D. Strekalov, R. Thompson, L. Baumgartel, I. Grudinin, and N. Yu, Opt. Express **19**, 14495 (2011).
[12] L. M. Baumgartel, R. J. Thompson, and N. Yu, Opt. Express **20**, 29798 (2012).
[13] J. D. Suter, I. M. White, H. Zhu, and X. Fan, Appl. Opt. **46**, 389 (2007).
[14] M. Han and A. Wang, Opt. Lett. **32**, 1800 (2007).
[15] L. He, Y.-F. Xiao, C. Dong, J. Zhu, V. Gaddam, and L. Yang, Appl. Phys. Lett. **93**, 201102 (2008).
[16] C. Xie, D. Cui, J. Tang, C. Shang, T. Zhang, C. Xue, and J. Liu, Micro Nano Lett. **9**, 609 (2014).
[17] Y. Zhi and A. Meldrum, Appl. Phys. Lett. **105**, 031902 (2014).
[18] S. Lane, F. Marsiglio, Y. Zhi, and A. Meldrum, Appl. Opt. **54**, 1331 (2015).
[19] H. Zhang and M. W. Grinstaff, Macromol. Rapid Commun. **35**, 1906 (2014).
[20] C. Lam, P. T. Leung, and K. Young, J. Opt. Soc. Am. B **9**, 1585 (1992).
[21] K. Takamura, H. Fischer, and N. R. Morrow, J. Pet. Sci. Eng. **98**, 50 (2012).
[22] F. Sedlmeir, R. Zeltner, G. Leuchs, and H. G. Schwefel, Opt. Express **22**, 30934 (2014).
[23] F. W. J. Olver and E. T. Goodwin, Math. Proc. Cambridge Philos. Soc. **48**, 414 (1952).
[24] I. Teraoka, S. Arnold, and F. Vollmer, J. Opt. Soc. Am. B **20**, 1937 (2003).
[25] M. Noto, D. Keng, I. Teraoka, and S. Arnold, Biophys. J. **92**, 4466 (2007).
[26] R. K. Mitra, S. S. Sinha, and S. K. Pal, Langmuir **23**, 10224 (2007).
[27] Z. Zhang, P. Zhao, P. Lin, and F. Sun, Polymer **47**, 4893 (2006).